

Research Paper

Cite this article: Wang H, Liu X, Yang X, Fang Z, Zhang R, Wang Y (2023). Penta-band rectangular slot antenna for multi-function wireless communication with linear and circular polarizations. *International Journal of Microwave and Wireless Technologies* **15**, 1382–1391. <https://doi.org/10.1017/S1759078722001489>

Received: 31 August 2022
Revised: 22 December 2022
Accepted: 22 December 2022







Key words:

Beidou navigation system; circularly polarization; c-type resonator; multi-band

Author for correspondence:

Xiaoming Liu,
E-mail: xiaoming.liu@ahnu.edu.cn

Penta-band rectangular slot antenna for multi-function wireless communication with linear and circular polarizations

Haiyang Wang¹ , Xiaoming Liu^{1,2} , Xiaofan Yang³ , Zhibin Fang² ,
Ran Zhang¹  and Ye Wang¹ 

¹The School of Physics and Electronic Information, Anhui Normal University, Wuhu 241002, China; ²Wuhu CEPREI Information Industry Technology Research Institute, Wuhu, Anhui 241002, China and ³The State Key Laboratory of Complex Electromagnetic Environment Effects on Electronic and Information System, Luoyang, Henan 471004, China

Abstract

This paper presents a multi-band rectangular slot antenna, which can be used in Beidou navigation system, 4G, WLAN and 5G system. The proposed antenna adopts a single feeding line, generating circular polarization for satellite navigation, and linear polarization for mobile communication systems. The proposed antenna consists of three c-type resonators and three rectangular loop slots. A c-type resonator and a rectangular loop slot work together to produce a usable frequency band. Multiple frequency bands can be generated by increasing the number of c-type resonator and rectangular loop slots. It is found that the c-type resonator changes the current distribution on the antenna surface, making the axial ratio less than 3 dB in the low frequency bands. Eventually, five operation frequency bands are realized. Experimentally, it is verified that the impedance bandwidths of each frequency band are 11.8% (1.12–1.26 GHz), 15.4% (1.5–1.75 GHz), 11.9% (2.36–2.66 GHz), 19.7% (3.15–3.84 GHz) and 2.6% (4.47–4.59 GHz), respectively. The measured 3 dB axial ratio bandwidths are 20 MHz at 1.2 and 1.56 GHz, fully covering BDS B1 and B2 bands. The measured gains are 3, 3.59, 4.07, 4.2 and 4.35 dBi, respectively.

Introduction

With the development of communication systems, more and more multi-band antennas are used in modern communication equipments [1]. There are many ways to achieve multi-band operation such as adding resonators [2–7], using multi monopoles or dipoles [8–13], etching slots [14–18], and so forth.

Many designs are based on the aforementioned methods. For instance, Luo *et al.* [5] designed a multi-band antenna by adding L-type branches exciting multiple modes. Cao *et al.* [6] used a T-shaped feeding patch to generate two frequency bands, and by adding stubs, a quad-band slot antenna was realized. Liu *et al.* [7] designed a quad-band antenna with the help of five-pointed star structure. These antennas provide multi-band operation by increasing the number of radiators. But they are not of circular polarization (CP).

For the multi monopole/dipole technique, there are also many designs. An antenna composed of three monopoles of different shapes was reported in [11]. The three monopoles worked together to generate three frequency bands, being useful for Bluetooth, 5G, and WLAN. Kasmaei *et al.* [12] designed a tri-band antenna by using monopoles and metamaterials. The impedance bandwidths are 25.8, 26.8 and 4.2%, which can be used for 3G, WiMAX and WLAN. Yang *et al.* [13] designed a quad-band magneto-electric (ME) dipole antenna by adding bent metal plats on the dipole. This is a good way to realize multi-band antenna. Unfortunately, the disadvantage lies in the difficulty of miniaturization. These antennas usually have relatively large size.

Etching slot method is another common method. Li *et al.* [17] introduced two slots of different shape on a circular patch, in this way a quad-band wearable patch antenna was realized. And the impedance bandwidths reach 3.67, 5.72, 5.85 and 9.74%, respectively. Ali *et al.* [18] designed a multi-band antenna by carving grooves on the ground plane, which could generate five frequency bands with impedance bandwidths of 11.5, 9.9, 13.4, 4 and 9.05%, respectively. Grooving on the ground layer is a good approach to design of multi-band antennas, but the impedance bandwidth of these antennas is not sufficiently wide.

There are also many other methods. For instance, using frequency selective surface (FSS), linearly polarized signals can be converted into circularly polarized signals. In this way, a quad-band antenna was designed [19]. Mao *et al.* designed multi-band antenna through coupled resonator network [20]. While achieving multi-band, these antennas also increase the complexity of the antenna structure.

Actually, there are three types of antenna polarization, linear polarization (LP), CP, and elliptical polarization [21, 22]. Circularly polarized antennas are widely used in global navigation satellite system due to orientation-independent characteristics, low multipath effect [23], and not affected by the Faraday rotation [24, 25]. Moreover, the dual-band circularly polarized antenna can improve the accuracy of positioning. In contrast, an LP antenna is relatively simpler than CP antenna to be realized [26]. Therefore, multi-frequency CP, especially the hybrid application design including CP and LP for different frequency band is even more challenging.

In this paper, a multi-band rectangular slot antenna for BDS/4G/WLAN/5G is proposed to combine both CP and LP to one single antenna. The antenna consists of three c-type resonators and three rectangular slots with different widths to generate five frequency bands at about 1.2, 1.56, 2.5, 3.6, 4.5 GHz. Multiple frequency bands can be generated by increasing the number of resonators and rectangular loop slots. The polarization mode of this antenna is right hand circular polarization (RHCP) in the BDS frequency bands, and LP in the 4G, WLAN, and 5G frequency bands. This multi-band antenna has a simple structure without needing of an additional feeding network, which is much preferred in wireless communication equipment.

Antenna design

The structure of the proposed antenna is illustrated in Fig. 1. The antenna consists of a 50-Ω microstrip feeding line, three c-type resonators, three rectangular loop slots with different widths and a rectangular slot under the feeding line. Three c-type resonate rings are printed on the top layer of a 1.6 mm thick FR4 substrate with a relative permittivity of 4.4 and a loss tangent of 0.02, while the three rectangular slots are etched on the bottom layer of

this substrate. The overall size of the antenna is $B \times B \times H$. To determine the final structure of the antenna, the antenna is modeled and simulated in the commercial software HFSS. The optimized dimensions of the proposed antenna are shown in Table 1.

The evolution of the multi-band antenna design is shown in Fig. 2. The AR and impedance bandwidth of Ant.1–Ant.4 are plotted in Fig. 3.

It is seen that Ant.1 consists of a 50-Ω microstrip feeding line, a c-type resonator and a rectangular loop slot, which can generate two frequency bands at about 1.2 and 2.1 GHz. The resonant frequency of the antenna is determined by the length of the resonant element and can be calculated according to the following equations. For Ant.1, the length of the resonant element can be written as

$$L_{b1} = B_1 + L_1 + w_1. \tag{1}$$

The corresponding resonant frequency can be estimated using

$$f_1 = \frac{c}{2 \times \sqrt{\epsilon_{eff}} \times L_{b1}}, \tag{2}$$

where c is the speed of light, and $\epsilon_{eff} = (\epsilon_r + 1)/2$. The calculated result reads $f_1 = 1.22 \text{ GHz}$, which is very close to the simulated results, where the first resonance takes place at 1.215 GHz. The equivalent circuit of Ant.1 is shown in Fig. 4. The antenna radiation element is represented by R_1 and L_1 . R_1 refers to the radiation loss of the antenna, L_1 stands for the inductance of the ring, C_1 denotes the terminal capacitor, and C_2 refers to the capacitor generated by the ground groove [12].

The axial ratio of Ant.1 is much greater than 3 dB and its polarization mode is LP. On the basis of Ant.1, a resonator and a rectangular slot are added and Ant.2 is formed. The second

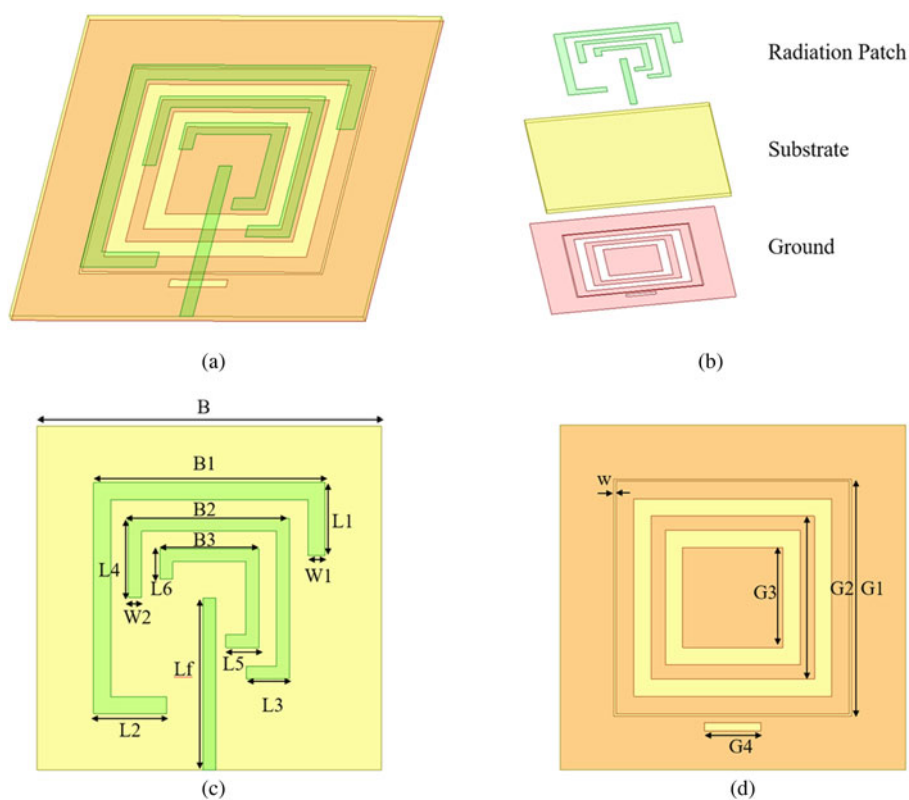


Fig. 1. Geometry of the proposed antenna. (a) 3D structure diagram; (b) Structural exploded diagram; (c) Radiation patch; (d) Ground plane.

Table 1. Dimension of the proposed antenna (unit: mm)

Parameter	Value	Parameter	Value
B	80	L_6	4.5
B_1	53.8	L_f	40
B_2	37.2	W	0.5
B_3	23	W_1	4
L_1	17	W_2	3
L_2	17	G_1	55
L_3	10	G_2	45.8
L_4	18.5	G_3	31.2
L_5	5.2	G_4	13

resonant frequency of Ant.2 is determined by the length of the second resonant element

$$L_{b_2} = B_2 \times 2 + L_3 + L_4 + w_2 \times 2. \tag{3}$$

By using

$$f_2 = \frac{c}{\sqrt{\epsilon_{\text{eff}}} \times L_{b_2}}, \tag{4}$$

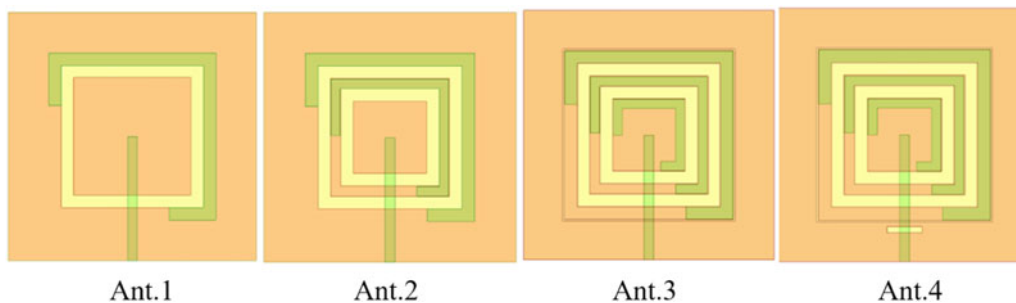


Fig. 2. The evolution process of the antenna.

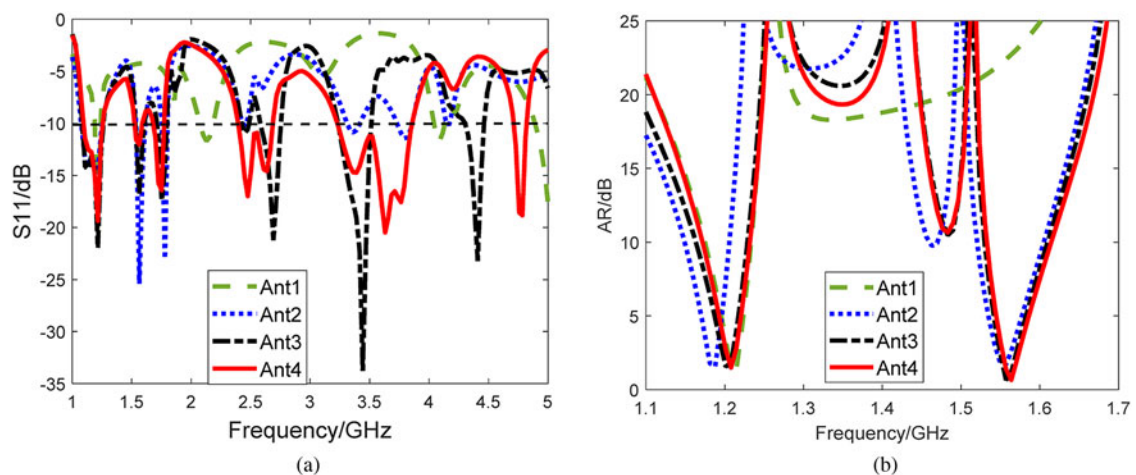


Fig. 3. Simulated S_{11} and AR for Ant.1- Ant.4. (a) S_{11} ; (b) AR.

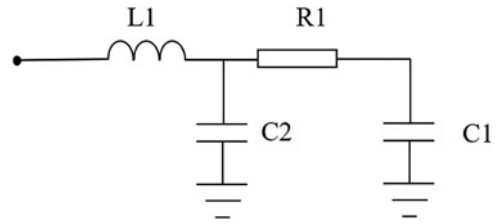


Fig. 4. Equivalent circuit for the c-type ring.

one obtains $f_2 = 1.68 \text{ GHz}$, which is also in the second range 1.50–1.75 GHz.

It can be seen from the simulation results that the reflection coefficient and the axial ratio are decreased. The axial ratio is less than 3 dB at 1.18 and 1.56 GHz, which can be applied to Beidou satellite navigation system (BDS). In order to increase the number of frequency bands, a small resonator on the inside and a rectangular slot with a width of w on the outermost side are added, see Ant.3. The axial bandwidth is shifted to the right, which can cover BDS B1 and B2 frequency bands. And the impedance bandwidth of the proposed antenna has been greatly improved. However, the impedance bandwidth is still a bit narrow and cannot fully cover WLAN and 5G frequency bands. Therefore, another rectangular slot on the ground is added to the antenna, see Ant.4. In this way, we obtain a multi-band rectangular slot antenna that can be used in BDS, 4G, WLAN, 5G.

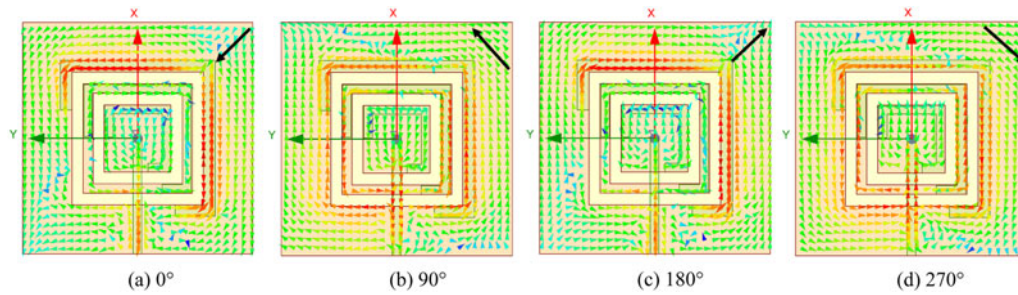


Fig. 5. Distribution diagram of antenna surface current changing with phase at 1.2 GHz. (a) 0°; (b) 90°; (c) 180°; (d) 270°.

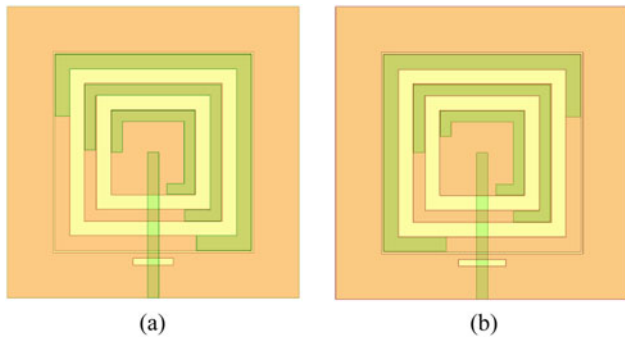


Fig. 6. Structure change of the antenna. (a) Initial structure; (b) Final structure.

The two frequency bands of Beidou satellite navigation system (BDS) are B1 1561.098 MHz and B2 1207.14 MHz, respectively. The c-type resonant unit affects the current distribution around the ring gap, generating two orthogonal polarization modes with a phase difference of 90° between *x* and *y* directions, thus exciting CP radiation. By adjusting the length of the c-type resonant unit, 3 dB axial ratio can be obtained. From the current distribution diagram, the sense of CP can be detected. The surface

current distributions of 0°, 90°, 180° and 270° at 1.2 GHz show in Fig. 5. It can be seen that the current rotates clockwise as the phase increases, indicating that the antenna radiates left-hand circularly polarized (LHCP) waves at 1.2 GHz.

The polarization mode of an antenna in satellite navigation system is right-handed circular polarization (RHCP). In order to adjust the polarization of the antenna to right-hand circular polarization, the first resonant ring is rotated by 90° as shown in Fig. 6(b). The current distribution of the antenna also changes after the modification. The current distributions of 0°, 90°, 180°, 270° at 1.2 GHz are plotted in Fig. 7(a). And the current distributions of 0°, 90°, 180°, 270° at 1.56 GHz is shown in Fig. 7(b). It can be found that the current rotates counterclockwise as the phase increases, implying that the antenna radiates right-hand circularly polarized (RHCP) waves at 1.2 and 1.56 GHz.

From the current distribution diagram, one can see the corresponding relationship between the antenna structure and the frequency band. The current is mainly distributed on the first resonator at 1.2 GHz, which means that the frequency band at 1.2 GHz is dominantly affected by the first resonator, being in line with equation (2). Similarly, the current is mainly distributed on the second resonator at 1.56 GHz.

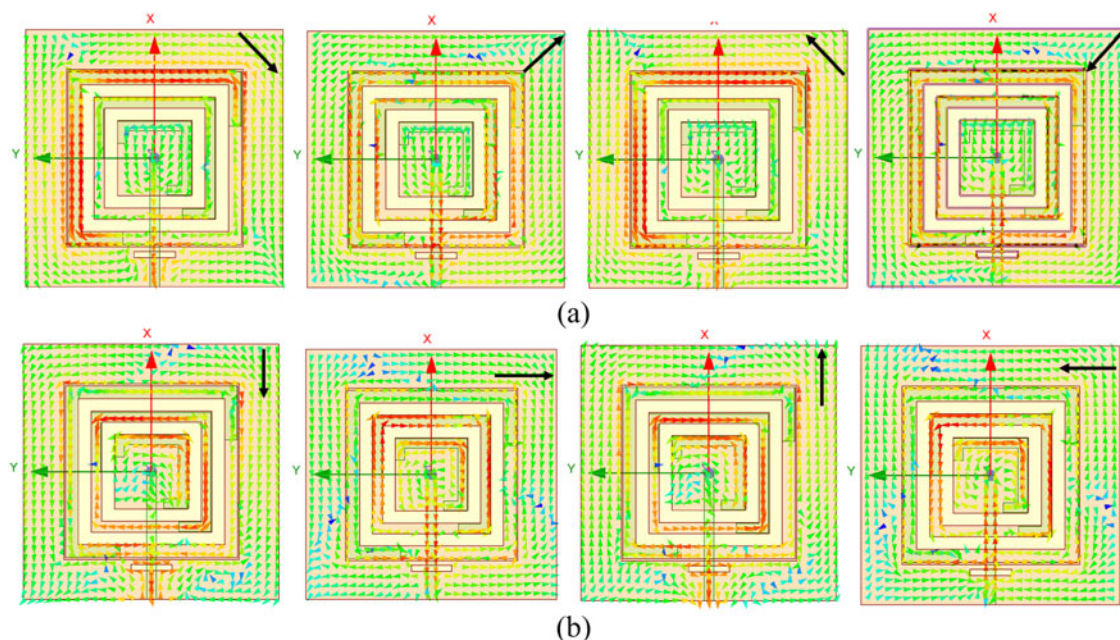


Fig. 7. Surface current distributions of the proposed antenna at (a) 1.2 GHz; (b) 1.56 GHz.

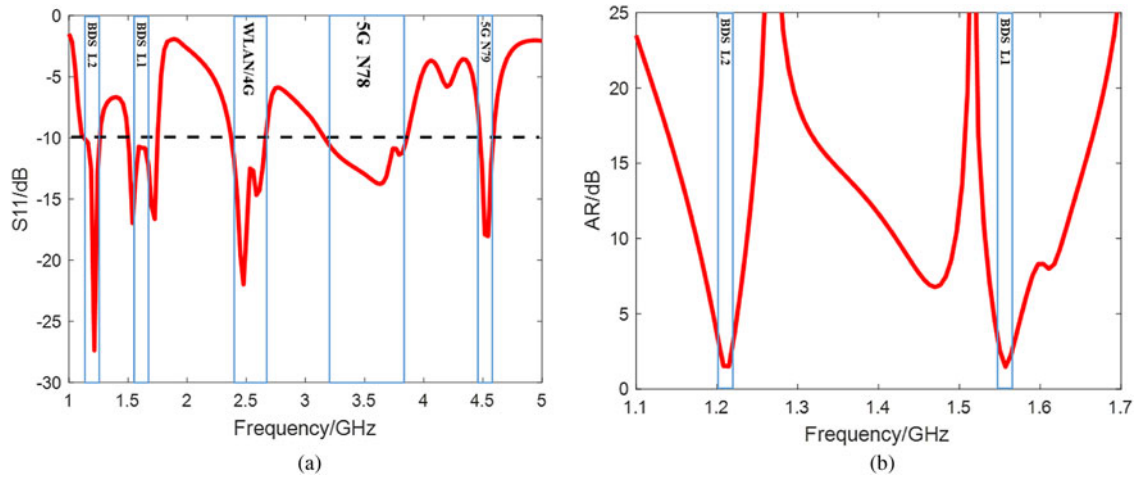


Fig. 8. The simulation result of the antenna. (a) S_{11} ; (b) AR.

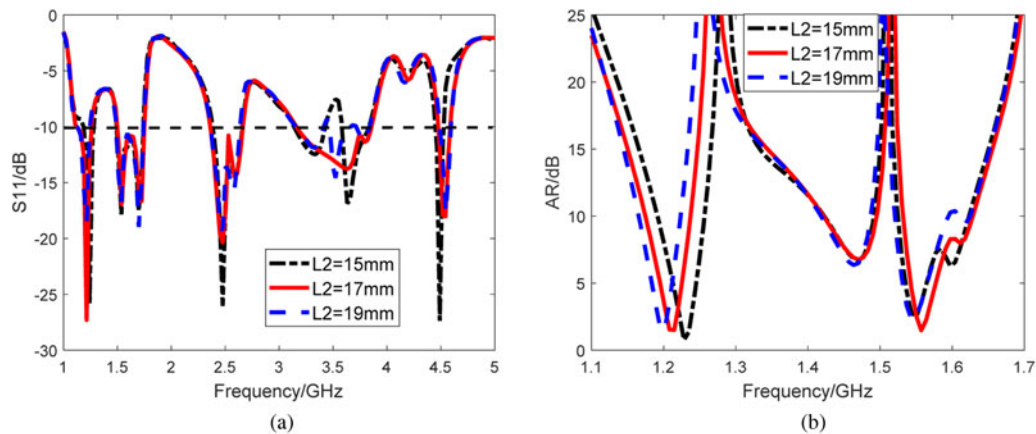


Fig. 9. Effect of L_2 on antenna performance. (a) S_{11} ; (b) AR.

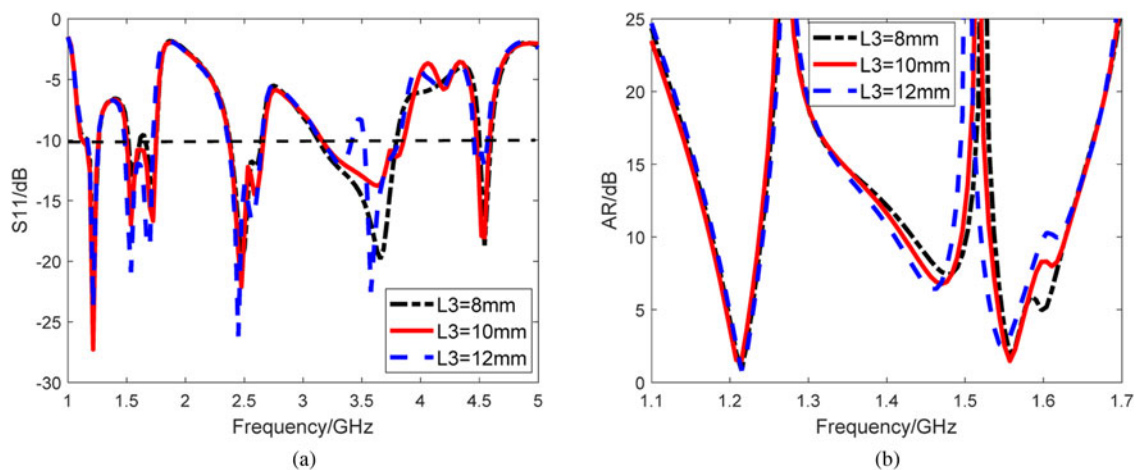


Fig. 10. Effect of L_3 on antenna performance. (a) S_{11} ; (b) AR.

The simulation results of the final structural are shown in Fig. 8. There are five frequency bands with reflection coefficient less than -10 dB, which is sufficiently good for BDS L_1 , BDS L_2 , 4G, WLAN and 5G. Moreover, the axial ratios in the BDS frequency bands are better than 3 dB.

Parameter study

From the evolution process, it is recognized that the number of frequency bands increases with the number of resonators and rectangular slots. Changing the length of the outermost resonators

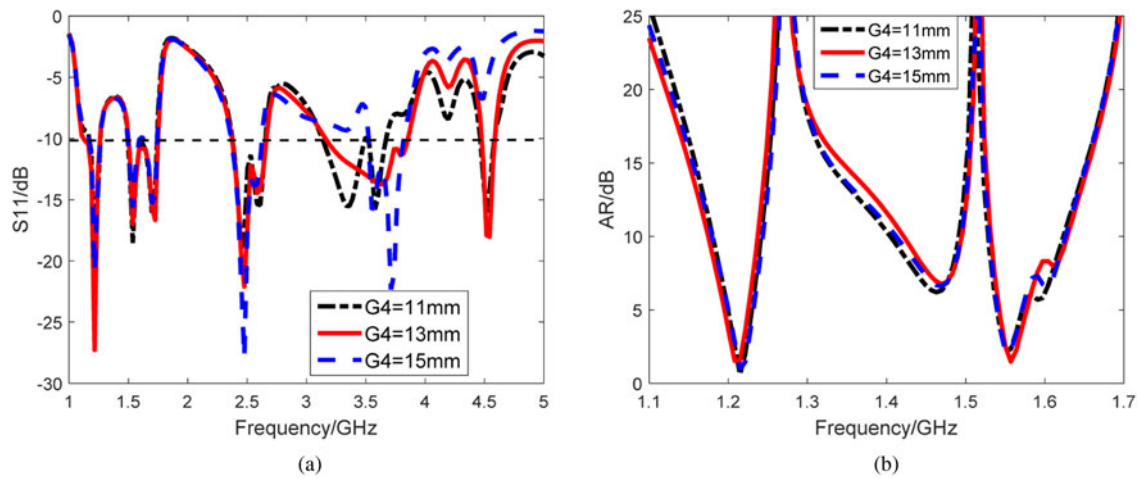


Fig. 11. Effect of G_4 on antenna performance. (a) S_{11} ; (b) AR.

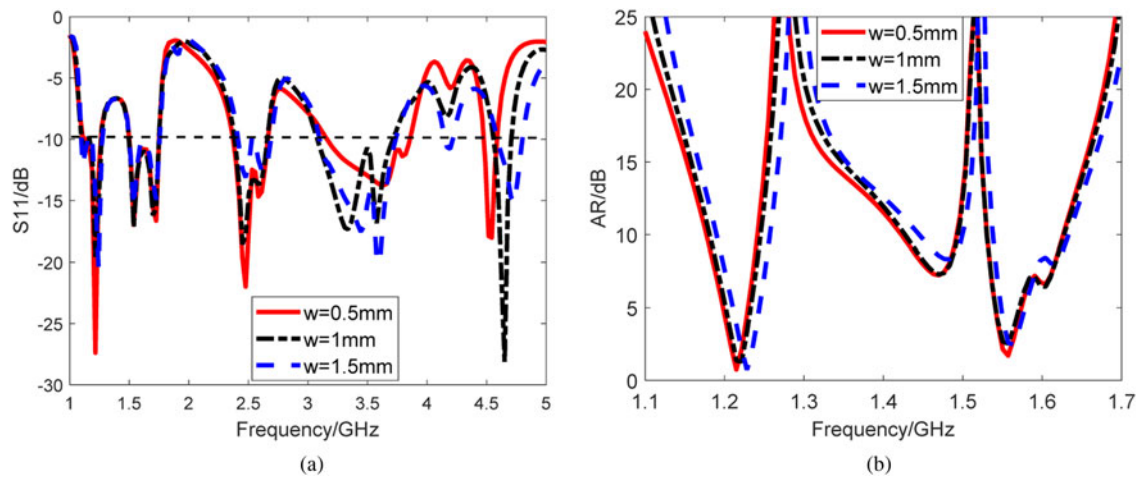


Fig. 12. Effect of w on antenna performance. (a) S_{11} ; (b) AR.

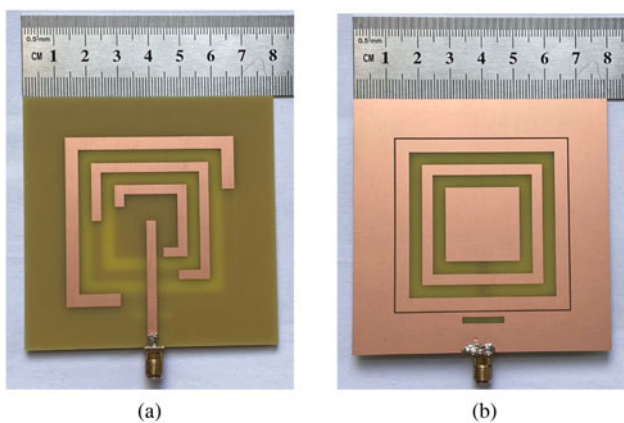


Fig. 13. Antenna real picture. (a) Top layer; (b) Bottom layer.

can generate two orthogonal modes with the same amplitude and a phase difference of 90° , realizing circularly polarized radiation. And the lowermost rectangular slot can significantly improve

the bandwidth of the multi-band antenna. Therefore, the parameters of the above structures are analyzed.

The first parameter sweep is performed on the length of the first resonator L_2 . The simulation results of reflection coefficient and axial ratio are shown in Fig. 9. From Fig. 9(a), one can see that the length of L_2 only affects the fourth frequency band. When L_2 becomes longer or shorter, the bandwidth of the fourth frequency band will become smaller. As shown in Fig. 9(b), with the length of L_2 increases the axial ratio frequency band shifts to the left. In addition, the axial ratio increase. In order to enable the fourth frequency band to fully cover the 5G N78 (3300–3800 MHz) band, while not compromising the performance of other CP bands, $L_2 = 17$ mm is chosen.

The simulation results of reflection coefficient and axial ratio versus the change of L_3 are plotted in Fig. 10. As L_3 increases, the reflection coefficient in the second frequency band becomes smaller, but the axial ratio becomes larger. And when $L_3 = 12$ mm, the impedance bandwidth of the fourth frequency band is decreased. Therefore, we choose $L_3 = 10$ mm to meet BDS and 5G requirements.

It is seen in the previous section that the rectangular slot also affects the impedance bandwidth. When $G_4 = 11$ mm, the

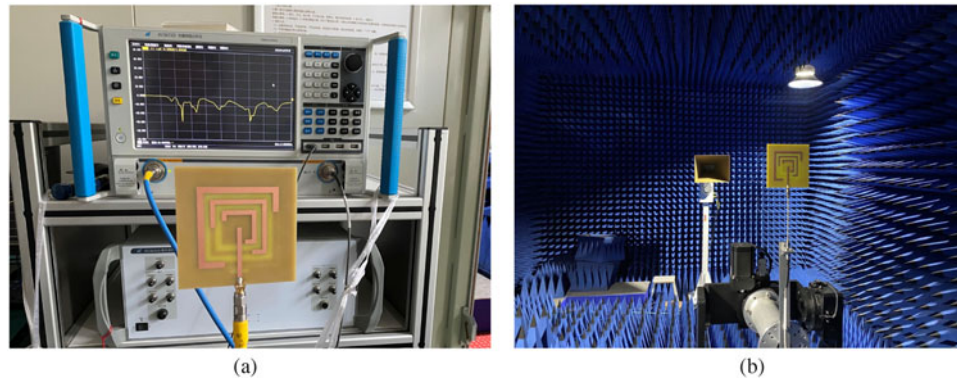


Fig. 14. Antenna measurement. (a) S_{11} ; (b) Far field.

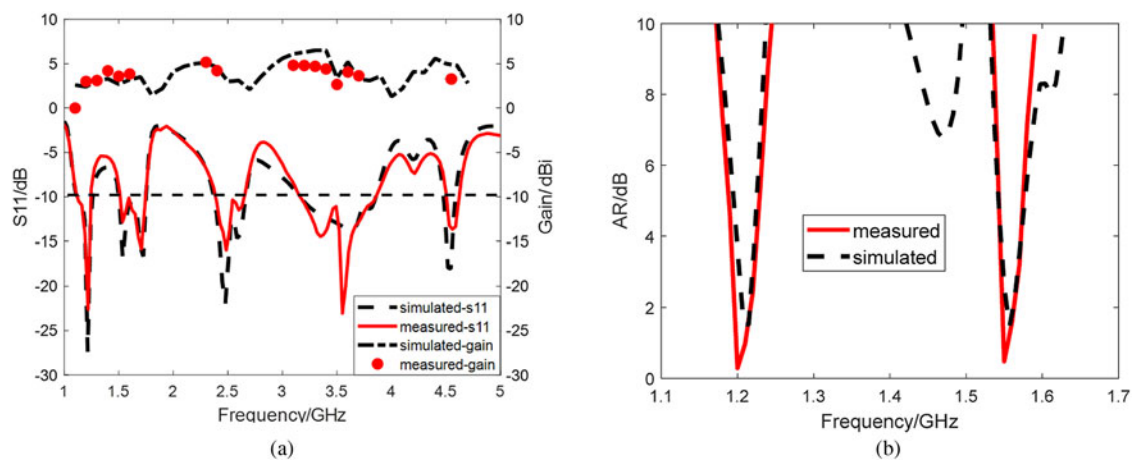


Fig. 15. Comparison of simulation and measured results. (a) S_{11} and Gain; (b) AR.

impedance bandwidth of the fourth frequency band is decreased. When $G_4 = 15$ mm, the antenna has only four frequency bands. From Fig. 11(b) it is seen that the length of G_4 has little effect on the axial ratio. Therefore, the size of rectangular slot is fixed at $G_4 = 13$ mm.

Finally, the width of the rectangular loop slot w is also studied, and the results are plotted in Fig. 12, where it is seen that w has similar effect on the impedance bandwidth as L_2 . When $w = 0.5$ mm, the impedance bandwidth is widest. As w increases the axial ratio frequency bands shift to the right. Adjusting the values of L_2 and w appropriately, one can get a suitable axial ratio over the operation frequency band.

Results and discussion

After optimization, the antenna is fabricated based on PCB technologies, as shown in Fig. 13.

The measurement on S_{11} is conducted using a calibrated vector network analyzer. And the far-field parameters and gain are measured in a microwave anechoic chamber (Fig. 14).

It can be seen from Fig. 15 that the simulated and measured impedance bandwidth, axial ratio bandwidth and gain are in good agreement with simulated ones. The measured impedance bandwidths at 1.2, 1.56, 2.5, 3.6 and 4.5 GHz are 11.8% (1.12–1.26 GHz), 15.4% (1.5–1.75 GHz), 11.9% (2.36–2.66 GHz), 19.7%

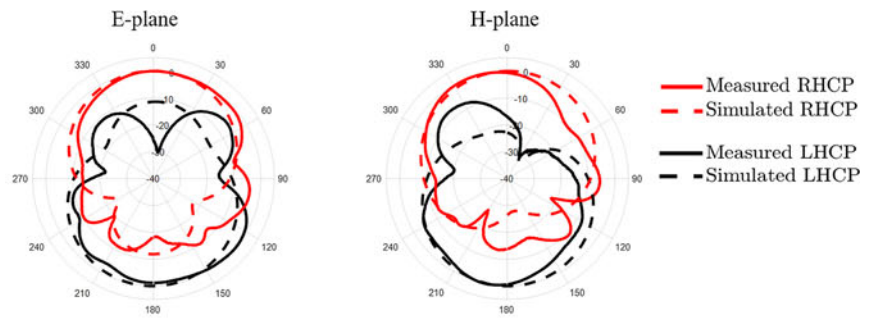
(3.15–3.84 GHz) and 2.6% (4.47–4.59 GHz), respectively. The measured 3 dB AR bandwidths are 20 MHz at 1.2 and 1.56 GHz, which can fully cover BDS B1 and B2 bands. The measured gains are 3, 3.59, 4.07, 4.2 and 4.35 dBi, respectively.

The antenna radiation patterns are shown in Fig. 16. For 1.2 and 1.56 GHz, circularly polarized radiation patterns are presented. As can be seen from Figs 16(a) and 16(b) the antenna radiates right-handed circularly polarized waves in the direction of wave propagation.

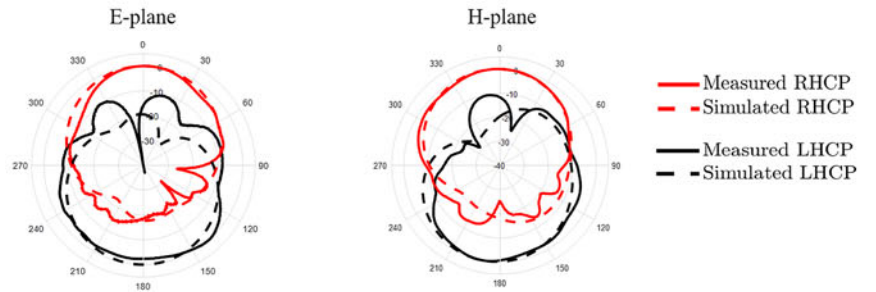
A comparison of this work with the designs in the literature is shown in Table 2. Compared with existing multi-band antennas, several merits of this design can be found. First, the antenna has five frequency bands and their bandwidths are wide enough, covering BDS, WLAN, 4G, 5G systems. Second, the antenna includes two polarization modes: LP and CP. The Beidou satellite navigation system requires the transmitting and receiving antennas to be circularly polarized. And the proposed antenna can well meet these requirements. In addition, in 4G, WLAN, and 5G frequency bands, the polarization modes of the antenna are LP. Third, this antenna is simple with low cost in fabrication.

Conclusion

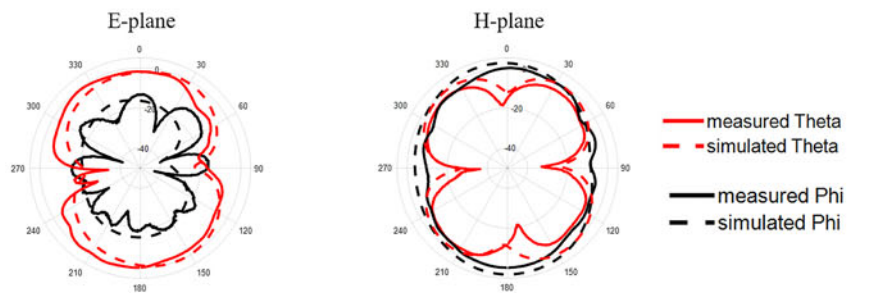
A multi-band microstrip antenna for BDS, 4G, WLAN, 5G applications was designed, fabricated and measured in this paper. CP is



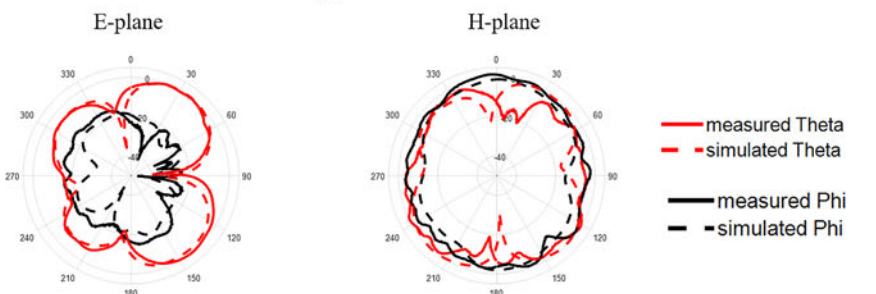
(a)



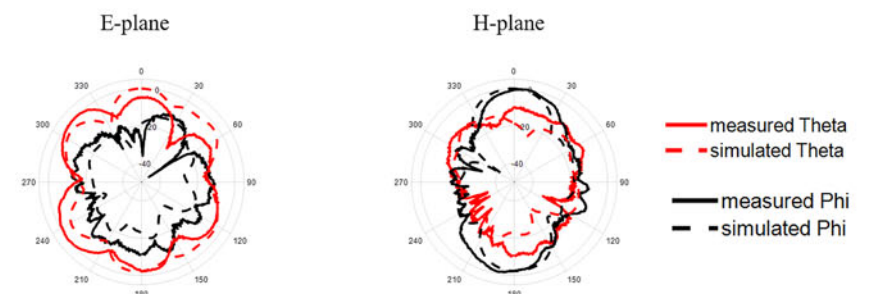
(b)



(c)



(d)



(e)

Fig. 16. The simulated and measured radiation patterns in *E* plane and *H* plane at (a) 1.2 GHz; (b) 1.56 GHz; (c) 2.5 GHz; (d) 3.6 GHz; (e) 4.5 GHz.

Table 2. Comparison of the multi-band antennas

Antenna	Antenna size (mm ³)	Number of frequency bands	$S_{11} < -10$ dB (%)	Measured gains (dBi)	Polarization	Cross-pol level (dB)
[6]	56 × 44 × 0.8	4	5.6, 5.9, 19.3, 13.7	3.55/3.93/5.02/4.86	LP	Not mentioned
[7]	90 × 60 × 0.127	4	23.9, 8.5, 4.3, 7.1	5.47/5.88/1.97/3.56	LP	-40/-40/-40/-60
[8]	28.3 × 20.3 × 1	3	15.4, 4.6, 7.9	4/3.8/2.7	LP	-20/-15/-30
[11]	24 × 19 × 1.53	3	5.8, 6.3, 6.6	2.26/3.14/3.73	LP	-10/-20/-25
[12]	45 × 40 × 1	3	25.8, 26.8, 4.2	2.23/2.81/1.91	LP	Not mentioned
[13]	100 × 100 × 40	4	3.2, 14.2, 11.1, 26.5	4.2/2.7/3.5/3.2	LP	-30/-40/-40/-40
[16]	35 × 30 × 1.6	4	3.58, 2.64, 2.5, 1.82	2.05/1.3/0.76/0.3	LP/CP	-25/-15/-15/-25
[17]	60 × 60 × 1.17	4	3.7, 5.7, 5.85, 9.8	-0.81/-2.81/-1.16/2.83	LP	-15/-15/-20/-10
[18]	35 × 30 × 1.6	5	11.5, 9.9, 13.4, 4, 9.05	3.9/3.7/1.13/ 2.16 /5.36	LP	Not mentioned
[19]	52 × 55 × 1.52	4	14.8, 80.7,	5.95/ 6.92/ 6.37/6.07	CP	-10/-15/-10/-20
[20]	50 × 50 × 2.626	4	1.2, 2, 1.9, 0.9	/	LP	-30/-40/-40/-30
This work	80 × 80 × 1.6	5	11.8, 15.4, 11.9, 19.7, 2.6	3/3.59/4.07/4.2/4.35	LP/CP	-10/-15/-15/-20/-20

achieved at 1.2 and 1.56 GHz by changing the length of the resonator. By increasing the number of the resonator and rectangular slots, multi-band operation is realized. The measured impedance bandwidths at 1.2, 1.56, 2.5, 3.6 and 4.5 GHz are 11.8, 15.4, 11.9, 19.7 and 2.6%, respectively. The measured 3 dB AR bandwidths are 20 MHz at 1.2 and 1.56 GHz, which can fully cover BDS B1 and B2 bands. A simple structure with a single feeding line is used to realize both CP and LP to a single antenna.

Data. Not applicable.

Acknowledgements. This work is funded in part by, the University Synergy Innovation Program of Anhui Province (GXXT-2021-027), the National Natural Science Foundation of China (61871003, 62101005), the Natural Science Foundation of Anhui province (No. 2108085QF256), the open project of the state key laboratory of complex electromagnetic environment effects on electronics and information system (CEMEE2022Z0201B) and Natural Science Research Project for Universities in Anhui Province (KJ2021A0101).

Author contributions. H. Wang and X. Yang did the design and simulation, Z. Fang and Y. Wang performed the measurement, R. Zhang plotted the figures, X. Liu prepared and reviewed the manuscripts, X. Liu, X. Yang, R. Zhang, and Y. Wang provided fundings.

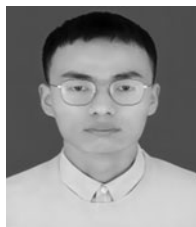
Conflict of interest. The authors report no conflict of interest.

References

- Wang S, Kong F, Li K and Du L (2021) A planar triple-band monopole antenna loaded with an arc-shaped defected ground plane for WLAN/WiMAX applications. *International Journal of Microwave and Wireless Technologies* **13**, 381–389.
- Qian J-F, Chen F-C, Xiang K-R and Chu Q-X (2019) Resonator-loaded multi-band microstrip slot antennas with bidirectional radiation patterns. *IEEE Transactions on Antennas and Propagation* **67**, 6661–6666.
- Xie Y, Chen F-C and Qian J-F (2020) Design of integrated duplexing and multi-band filtering slot antennas. *IEEE Access* **8**, 126119–126126.
- Sharma M (2019) Design of multiband circularly/linearly polarized antenna for multiple wireless (WWAN/Bluetooth/WiMAX/WLAN/Downlink Satellite System). *International Journal of Microwave and Wireless Technologies* **11**, 967–974.
- Luo Y, Zhu L, Liu Y, Liu N and Gong S (2021) Multi-band monopole smartphone antenna with bandwidth enhancement under radiation of multiple same-order modes. *IEEE Transactions on Antennas and Propagation* **70**, 2580–2592. doi: <https://doi.org/10.1109/TAP.2021.3125364>.
- Cao YF, Cheung SW and Yuk TI (2015) A multiband slot antenna for GPS/WiMAX/WLAN systems. *IEEE Transactions on Antennas and Propagation* **63**, 952–958.
- Liu HW, Wen P, Zhu SS, Ren BP, Guan XH and Yu H (2015) Quad-band CPW-fed monopole antenna based on flexible pentangle-loop radiator. *IEEE Antennas and Wireless Propagation Letters* **14**, 1373–1376.
- Xu KD, Li D, Liu Y and Liu QH (2018) Printed quasi-yagi antennas using double dipoles and stub-loaded technique for multi-band and broadband applications. *IEEE Access* **6**, 31695–31702.
- Cui J, Zhang A and Chen X (2020) An omnidirectional multiband antenna for railway application. *IEEE Antennas and Wireless Propagation Letters* **19**, 54–58.
- Zhang J, Yang K, Eide E, Yan S and Vandenbosch GAE (2020) Simple triple-mode dual-polarized dipole antenna with small frequency separation ratio. *IEEE Antennas and Wireless Propagation Letters* **19**, 262–266.
- Sreelakshmi K, Rao GS and Kumar MNVSS (2020) A compact grounded asymmetric coplanar strip-fed flexible multiband reconfigurable antenna for wireless applications. *IEEE Access* **8**, 194497–194507.
- Kasmaei M, Zareian-Jahromi E, Basiri R and Mashayekhi V (2022) Miniaturized triple-band monopole antenna loaded with a via-less MTM for 3G, WiMAX, and WLAN applications. *International Journal of Microwave and Wireless Technologies* **14**, 601–608.
- Yang G, Zhang S, Li J, Zhang Y and Pedersen GF (2020) A multi-band magneto-electric dipole antenna with wide beam-width. *IEEE Access* **8**, 68820–68827.
- Hsu C-K and Chung S-J (2014) Compact antenna with U-shaped open-end slot structure for multi-band handset applications. *IEEE Transactions on Antennas and Propagation* **62**, 929–932.
- Lu J-H and Huang B-J (2013) Planar compact slot antenna with multi-band operation for IEEE 802.16m application. *IEEE Transactions on Antennas and Propagation* **61**, 1411–1414.
- Singh G, Kanaujia BK, Pandey VK and Kumar S (2022) Quad-band multi-polarized antenna with modified electric-inductive – capacitive resonator. *International Journal of Microwave and Wireless Technologies* **14**, 65–76.
- Li H, Du J, Yang X-X and Gao S (2022) Low-profile all-textile multiband microstrip circular patch antenna for WBAN applications. *IEEE Antennas and Wireless Propagation Letters* **21**, 779–783.
- Ali T, Fatima N and Biradar RC (2018) A miniaturized multiband reconfigurable fractal slot antenna for GPS/GNSS/Bluetooth/WiMAX/X-band

applications. *AEU – International Journal of Electronics and Communications* **94**, 234–243.

19. **Hoang TV, Le TT, Li QY and Park HC** (2016) Quad-band circularly polarized antenna for 2.4/5.3/5.8-GHz WLAN and 3.5-GHz WiMAX applications. *IEEE Antennas and Wireless Propagation Letters* **15**, 1032–1035.
20. **Mao C-X, Gao S, Wang Y and Sanz-Izquierdo B** (2017) A novel multi-band directional antenna for wireless communications. *IEEE Antennas and Wireless Propagation Letters* **16**, 1217–1220.
21. **Zhu HL, Cheung SW, Liu XH and Yuk TI** (2014) Design of polarization reconfigurable antenna using metasurface. *IEEE Transactions on Antennas and Propagation* **62**, 2891–2898.
22. **Ni C, Chen MS, Zhang ZX and Wu XL** (2018) Design of frequency-and polarization-reconfigurable antenna based on the polarization conversion metasurface. *IEEE Antennas and Wireless Propagation Letters* **17**, 78–81.
23. **Sharma A, Das G, Gupta S and Gangwar RK** (2020) Quad-band quadrise circularly polarized dielectric resonator antenna for GPS/CNSS/WLAN/WiMAX applications. *IEEE Antennas and Wireless Propagation Letters* **19**, 403–407.
24. **Feng G, Chen L, Xue X and Shi X** (2017) Broadband circularly polarized crossed-dipole antenna with a single asymmetrical cross-loop. *IEEE Antennas and Wireless Propagation Letters* **16**, 3184–3187.
25. **Zhong Z-P, Zhang X, Liang J-J, Han C-Z, Fan M-L, Huang G-L, Xu W and Yuan T** (2019) A compact dual-band circularly polarized antenna with wide axial-ratio beamwidth for vehicle GPS satellite navigation application. *IEEE Transactions on Vehicular Technology* **68**, 8683–8692.
26. **Singh HS, Agarwal M, Pandey GK and Meshram MK** (2014) A quad-band compact diversity antenna for GPS L1/Wi-Fi/LTE2500/WiMAX/HIPERLAN1 applications. *IEEE Antennas and Wireless Propagation Letters* **13**, 249–252.



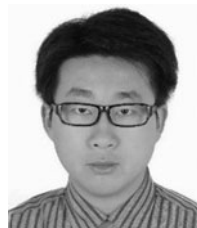
Haiyang Wang received the bachelor's degree in electronic information engineering from Anhui Normal University, Wuhu, Anhui, China, in 2020. He is currently pursuing the degree with the School of Physics and Electronic Information, Anhui Normal University, Wuhu, China. His research focuses on circular polarized antenna design.



He is now with the School of Physics and Electronic Information, Anhui Normal University. His research interests include terahertz science and

Xiaoming Liu received the B.Sc. degree in applied physics in Nanjing University of Posts and Telecommunications in 2006, Nanjing, China, and Ph.D. degree in 2012 in electronic engineering at the School of Electronic Engineering and Computer Science, Queen Mary University of London, London, UK. In 2012, he joined the School of Electronic Engineering, Beijing University of Posts and Telecommunications.

technology, quasi-optical techniques and systems, millimeter and sub-millimeter wave antenna measurement techniques and bio-electromagnetics.



Xiaofan Yang received the Ph.D. degree in 2012 in electromagnetic and microwave technology at the School of Electronic Science and Engineering, University of Electronic Science and Technology of China. During the period as a doctoral student, he joined the EHF Key Laboratory of Fundamental Science, University of Electronic Science and Technology of China. From 2011 to 2012, he has been titled as visiting scientist to RAL Space, Rutherford Appleton Laboratory, Science and Technology Facilities Council, at Oxford, UK. He is now with the State Key Laboratory of Complex Electromagnetic Environment Effects on Electronics and Information System, Luoyang Electronic Equipment Test Center of China. His research interests include terahertz science and technology, electromagnetic wave propagation, millimeter and sub-millimeter wave receiver front-end.



and Reliability, Automatic control, Intelligent manufacturing and bioelectro-magnetics.

Zhibin Fang, Senior Engineer, received the B.Sc. degree in automation major in Guangdong University of Technology in 2003, China, and Master of Science in Engineering in 2020 in School of Business Administration, South China University of Technology, China. He is now working in China Electronic Product Reliability and Environmental Testing Research Institute. His research interests include Quality



massive MIMO, intelligent reflecting surface and signal processing.

Ran Zhang received the B.S. degree in internet of things engineering from the Hebei University of Engineering, Hebei, China, in 2016, and the Ph.D. degree in information and communication engineering from Beijing University of Posts and Telecommunications, Beijing, China, in 2021. She is now working with Anhui Normal University. Her current research interests include millimeter wave communications,



millimeter wave circuits, optimization algorithms, and massive MIMO systems.

Ye Wang received the B.Eng. degree in electronic science and technology from Tianjin University, Tianjin, China, in 2010, and the M.Eng. degree from the University of Melbourne, Melbourne, Australia, in 2013. He obtained his Ph.D. degree from Beijing University of Posts and Telecommunications, Beijing, China, in 2020. He is now working with Anhui Normal University. His research interests include milli-